Therapeutic Efficacy of a ^{188}Re-Labeled α-Melanocyte–Stimulating Hormone Peptide Analog in Murine and Human Melanoma-Bearing Mouse Models

Yubin Miao, PhD[1,2]; Nellie K. Owen, DVM[3]; Darrell R. Fisher, PhD[4]; Timothy J. Hoffman, PhD[2,5]; and Thomas P. Quinn, PhD[1,3]

[1]Department of Biochemistry, University of Missouri-Columbia, Columbia, Missouri; [2]Department of Internal Medicine, University of Missouri-Columbia, Columbia, Missouri; [3]Department of Radiology, University of Missouri-Columbia, Columbia, Missouri; [4]Pacific Northwest National Laboratory, Richland, Washington; and [5]Harry S. Truman Memorial Veteran Hospital, Columbia, Missouri

The purpose of this study was to examine the therapeutic efficacy of ^{188}Re-(Arg^{11})[Cys^{3,4,10},D-Phe^7]α-melanocyte–stimulating hormone$_{3–13}$ (CCMSH) in the B16/F1 murine melanoma- and TXM13 human melanoma-bearing mouse models. **Methods:** (Arg^{11})CCMSH was synthesized and labeled with ^{188}Re to form ^{188}Re-(Arg^{11})CCMSH. B16/F1 melanoma-bearing mice were administrated 7.4 MBq, 22.2 MBq, and 2 × 14.8 MBq of ^{188}Re-(Arg^{11})CCMSH via the tail vein. TXM13 melanoma-bearing mice were separately injected with 22.2 MBq, 2 × 14.8 MBq, and 37.0 MBq of ^{188}Re-(Arg^{11})CCMSH through the tail vein. Two groups of 10 mice bearing either B16/F1 or TXM13 tumors were injected with saline as untreated controls. **Results:** In contrast to the untreated control group, ^{188}Re-(Arg^{11})CCMSH yielded rapid and lasting therapeutic effects in the treatment groups with either B16/F1 or TXM13 tumors. The tumor growth rate was reduced and the survival rate was prolonged in the treatment groups. Treatment with 2 × 14.8 MBq of ^{188}Re-(Arg^{11})CCMSH significantly extended the mean life of B16/F1 tumor mice ($P < 0.05$), whereas the mean life of TXM13 tumor mice was significantly prolonged after treatment with 22.2-MBq and 37.0- MBq doses of ^{188}Re-(Arg^{11})CCMSH ($P < 0.05$). High-dose ^{188}Re-(Arg^{11})CCMSH produced no observed normal tissue toxicity. **Conclusion:** The therapy study results revealed that ^{188}Re-(Arg^{11})CCMSH yielded significant therapeutic effects in both B16/F1 murine melanoma- and TXM13 human melanoma-bearing mouse models. ^{188}Re-(Arg^{11})CCMSH appears to be a promising radiolabeled peptide for targeted radionuclide therapy of melanoma.

Key Words: α-melanocyte–stimulating hormone; ^{188}Re-labeled peptide; targeted radionuclide therapy; human melanoma; murine melanoma

J Nucl Med 2005; 46:121–129

Malignant melanoma is the sixth most commonly diagnosed cancer in the United States, where 55,100 cases of malignant melanoma will be newly reported and 7,910 fatalities will occur in the year 2004 (*1*). Melanoma metastases are difficult to treat because metastatic melanoma deposits are resistant to conventional chemotherapy and external beam radiation therapy (*2*). Moreover, melanoma metastases are aggressive, and the average survival for patients with metastatic melanoma is only ~6–9 mo (*3*). Therefore, it is crucial to develop effective novel agents for early detection and treatment of primary lesions and their metastases.

The use of radiolabeled receptor-mediated peptide analogs for the treatment of primary and metastatic tumors—namely, targeted radionuclide therapy—has been an important alternative to conventional therapeutic regimens. Receptor-avid peptides have been chosen as vehicles to selectively deliver cytotoxic radiation-emitting radionuclides to tumor cells, resulting in tumor cell death (*4*). In comparison with external beam radiation therapy and chemotherapy, targeted radionuclide therapy can specifically deliver the radiation dose to tumor cells, while sparing the normal tissues and organs. Auger electron–emitting, α-particle–emitting, and β-particle–emitting radioisotopes may be used to label receptor-avid peptides for targeted radionuclide therapy (*5*). Several β-particle–emitting radioisotopes, such as ^{131}I, ^{188}Re, ^{90}Y, and ^{177}Lu, are being used for targeted tumor radiotherapy (*6–11*). High-energy β-emitters such as ^{188}Re and ^{90}Y appear appropriate for the treatment of larger tumor burdens. Medium- and lower-energy β-emitters, such as ^{153}Sm and ^{177}Lu, may be more suitable for treating smaller tumors or metastatic deposits. Radiolabeled peptides with high receptor affinities have been successfully used in somatostatin receptor–positive tumor de-

tection and therapy (6–9,12–18). For instance, impressive therapeutic efficacy studies of ^{90}Y-DOTA-Tyr^3-octreotide (DOTA is 1,4,7,10-tetraazacyclododecane-N,N',N'',N'''-tetraacetic acid) have been reported (6,7), and the ^{90}Y-labeled octreotide analog is currently in clinical trials to treat somatostatin receptor–positive tumors (15–18). ^{177}Lu-DOTA-Y3-octreotate is another promising agent for treating somatostatin receptor–positive tumors (9). Significant advances in the use of radiolabeled peptides for cancer therapy make targeted radionuclide therapy attractive as a treatment modality for cancer.

At the present time, some of the most promising agents for melanoma targeting are α-melanocyte–stimulating hormone (α-MSH) peptide analogs. The presence of α-MSH receptors on both human and mouse melanoma cells suggests that α-MSH peptide analog may be used as a vehicle to selectively deliver different radionuclides to target tumor cells for melanoma imaging and therapy (19–22). Several α-MSH peptides, based on the super potent [Nle^4,D-Phe^7]α-MSH (NDP) analog (23), have been examined for their abilities to target melanoma (24–27). Further chemical modification of NDP sequence resulted in ^{111}In-DOTA-MSH$_{oct}$ and ^{111}In-DOTA NAPamide, a class of 8-amino-acid peptides with melanoma imaging potential due to their rapid uptake and clearance properties (28,29). Over the past several years, our laboratory has developed a novel class of metal-cyclized α-MSH peptide analogs for melanoma imaging and therapy (30–34). Metal-mediated peptide cyclization made the molecule resistant to chemical and proteolytic degradation in vivo while retaining high bioactivities. ^{188}Re-(Arg^{11})[Cys^{3,4,10},D-Phe^7]α-melanocyte–stimulating hormone$_{3–13}$ (CCMSH) exhibited favorable tumor-targeting properties and pharmacokinetics in both murine and human melanoma-bearing mouse models, which highlighted its potential as a therapeutic agent (33,34).

^{188}Re is an attractive radioisotope for targeted radionuclide therapy because of its high-energy β-particle emission ($E_{\beta max}$ = 2.11 MeV), short half-life (16.95 h), and commercial availability (35). Moreover, the decay of ^{188}Re yields a 155- keV γ-emission (15% abundance), which allows tumor imaging during therapy using standard nuclear medicine imaging systems optimized for ^{99m}Tc. In the current article, we report an investigation into the therapeutic potential of ^{188}Re-(Arg^{11})CCMSH in both the B16/F1 murine melanoma-bearing C57 mouse model and TXM13 human melanoma xenografted SCID (severe combined immunodeficiency) mouse model. The administration of ^{188}Re-(Arg^{11})CCMSH exhibited significant therapeutic effects in both B16/F1 murine melanoma- and TXM13 human melanoma-bearing mouse models.

MATERIALS AND METHODS

Chemicals and Reagents

Amino acids and resin were purchased from Advanced ChemTech Inc. ^{188}ReO$_4^-$ was obtained from a ^{188}W/^{188}Re generator at Oak Ridge National Laboratory. All chemicals used in this study were purchased from Fischer Scientific and were used without further purification. The B16/F1 murine melanoma cell line was obtained from American Tissue Culture Collection and the TXM13 human melanoma cell line was supplied by Dr. Isaiah J. Fidler and Dr. Janet Price (Cell Biology Department, University of Texas, M.D. Anderson Cancer Center, Houston, TX).

Preparation of ^{188}Re-(Arg^{11})CCMSH

The α-MSH peptide analog, (Arg^{11})CCMSH, was synthesized by a method previously described (33). The identity of peptide was confirmed by electrospray ionization mass spectrometry (Mass Consortium Corp.). ^{188}Re-(Arg^{11})CCMSH was prepared via a modified glucoheptonate transchelation reaction (33). Briefly, fresh ^{188}ReO$_4^-$ elution (1.85 GBq) was evaporated under N$_2$ gas to dryness in a reaction vial. Six hundred microliters of 6 mg/mL SnCl$_2$ in 0.2 mol/L sodium glucoheptonate aqueous solution were added into the reaction vial. The mixture was incubated at 75°C for 30 min to form ^{188}Re-glucoheptonate. To the mixture, 10 μL of a 1 mg/mL (Arg^{11})CCMSH aqueous solution were added. After adjusting the pH to 8.5 with 1 mol/L NaOH, the resulting solution was incubated at 75°C for 30 min. The ^{188}Re cyclized peptide was purified to a single species by high-performance liquid chromatography (HPLC) on a C$_{18}$ reversed-phase column. A 20-min gradient of 18%–28% acetonitrile in H$_2$O/20 mmol/L HCl was used to separate the ^{188}Re-labeled peptide from excess nonlabeled peptide. Before the collection, 25 mg of L-ascorbic acid were added into the collection vial to eliminate the radiolysis and reoxidation of ^{188}Re-(Arg^{11})CCMSH. Stability of the therapeutic dose level of ^{188}Re-(Arg^{11})CCMSH was monitored up to 24 h for degradation by HPLC. Purified ^{188}Re-labeled peptide sample was purged with N$_2$ gas for 20 min to remove the acetonitrile. The pH of final solution was adjusted to 5 with 1 mol/L NaOH and normal saline for dose administration.

Dosimetry Studies

All animal studies were conducted in compliance with the Institutional Animal Care and Use Committee approval. The biodistribution of ^{188}Re-(Arg^{11})CCMSH was assessed at 5 min, 30 min, and 1, 4, 24, and 48 h in B16/F1 murine melanoma-bearing C57 mice (6–7 wk old; Harlan) to evaluate radiation-absorbed doses from ^{188}Re-(Arg^{11})CCMSH in tumor and normal organs and tissues by using methods described previously (36,37). Groups of 5 mice per each time point were used for the biodistribution studies. Each mouse was injected through the tail vein with 0.111 MBq (2.72×10^{-11} g) of ^{188}Re-(Arg^{11})CCMSH for the 5-min, 30-min, 1-h, and 4-h time points. For the 24- and 48-h time points, 0.333 MBq (8.16×10^{-11} g) and 1.184 MBq (2.90×10^{-10} g) of ^{188}Re-(Arg^{11})CCMSH were injected into each mouse via the tail vein. Time–activity curves were generated for 13 organs and tissues (blood, brain, heart, lung, liver, spleen, stomach, kidney, large intestine, small intestine, muscle, pancreas, and tumor). Cumulative activities were determined for each organ by integrating the area under the time–activity curves. The cumulative activities were then used with a dosimetric model (36) developed specifically for the laboratory mouse. The dosimetric model is used to evaluate dose from activity within tissues as well as the cross-organ β-dose contributions.

Scintigraphic Melanoma Imaging of [188]Re-(Arg[11])CCMSH

Two B16/F1 melanoma-bearing C57 mice were injected with 5.55 MBq (1.36×10^{-9} g) and 11.1 MBq (2.72×10^{-9} g) of [188]Re-(Arg[11])CCMSH via the tail vein, respectively. The mice were sacrificed at 4 and 18 h after injection, and γ-scintigraphic imaging of melanoma-bearing mice was performed using a Siemens low-energy mobile γ-camera equipped with a low-energy, parallel-hole collimator. The planar images were collected on a 512 matrix with 1.5× magnification and 8-bit depth.

Radionuclide Therapy of [188]Re-(Arg[11])CCMSH

The therapeutic efficacy of [188]Re-(Arg[11])CCMSH was examined in B16/F1 murine melanoma-bearing C57 mice. C57 mice were inoculated subcutaneously with 1×10^6 B16/F1 murine melanoma cells in the right flank. Palpable dark melanoma tumors were observed 3 d after tumor cell inoculation. Three treatment groups of 10 mice were administrated a single dose of 7.4 MBq (1.81×10^{-9} g), 22.2 MBq (5.44×10^{-9} g), or 2×14.8 MBq ($2 \times 3.63 \times 10^{-9}$ g) of [188]Re-(Arg[11])CCMSH (3 d apart) through the tail vein on the fourth day after tumor cell implantation. An untreated control group received 100 μL of normal saline. SCID mice received subcutaneous bilateral flank inoculations of 5×10^6 TXM13 human melanoma cells per site. Measurable tumors were obtained 7 wk after inoculation. Three treatment groups of 10 mice were administered 22.2 MBq (5.44×10^{-9} g), 2×14.8 MBq ($2 \times 3.63 \times 10^{-9}$ g) (2 wk apart), and 37.0 MBq (9.07×10^{-9} g) of [188]Re-(Arg[11])CCMSH through the tail vein on the fourth day after the observance of measurable tumors. An untreated control group received 100 μL of normal saline. In parallel with therapeutic dose administration, HPLC analysis was performed to confirm the purity of [188]Re-(Arg[11])CCMSH. In addition, 2 B16/F1 melanoma-bearing mice were injected with 0.111 MBq of [188]Re-(Arg[11])CCMSH through the tail vein and sacrificed at 1 h after injection to confirm the bioactivity of [188]Re-(Arg[11])CCMSH. After the administration of the therapeutic infusion, tumor size was determined daily for B16/F1 tumors and twice a week for TXM13 tumor*s* by measuring the length, the width, and the depth of tumor with a caliper. Tumor volume was calculated by using the follow-

ing formula: tumor volume = (length × width × depth) × π/6. Animal body condition and body weight were determined daily for B16/F1 tumor-bearing mice and twice a week for TXM13 tumor-bearing mice. Hematologic toxicity of [188]Re-(Arg[11])CCMSH was determined in TXM13 tumor-bearing mice treated with 37.0 MBq of [188]Re-(Arg[11])CCMSH. Twenty microliters of blood were collected from the vein in the flank of each mouse by using an ethylenediaminetetraacetic acid–coated capillary tube. White blood cell (WBC), red blood cell (RBC), and platelet counts were performed by a hematology analyzer before therapy and at weekly intervals thereafter for 6 wk. Mice were removed from the therapy study and sacrificed if the body weight loss was >20% of initial body weight, the tumor size exceeded 1.0 cm³, or skin ulcerations appeared at the tumor site. Toxicity of [188]Re-(Arg[11])CCMSH to vital organs, such as kidney, heart, liver, and stomach, was evaluated by pathologic examination after completion of the therapy study. After decay of [188]Re, excised organs were examined by a pathologist at the University of Missouri School of Veterinary Medicine Research Animal Diagnostic Laboratory. Kaplan–Meier survival curves were obtained by using SPSS software (SPSS Inc.). Statistical analysis was performed using the Student *t* test for unpaired data. A 95% confidence level was chosen to determine the significance between the untreated and treated groups, with $P < 0.05$ considered significantly different.

RESULTS

The peptide (Arg[11])CCMSH was synthesized, purified by reversed-phase HPLC (RP-HPLC), and its identity was confirmed by electrospray ionization mass spectrometry. An illustration of the [188]Re-(Arg[11])CCMSH structure is shown in Figure 1. (Arg[11])CCMSH was labeled with [188]Re through a glucoheptonate transchelation reaction, using stannous chloride as a reducing agent. [188]Re-(Arg[11])CCMSH was separated completely from its nonlabeled counterpart by RP-HPLC. The addition of L-ascorbic acid eliminated radiolysis and reoxidation of [188]Re-(Arg[11])CCMSH. A therapeutic dose of [188]Re-(Arg[11])CCMSH was stable for 24 h at
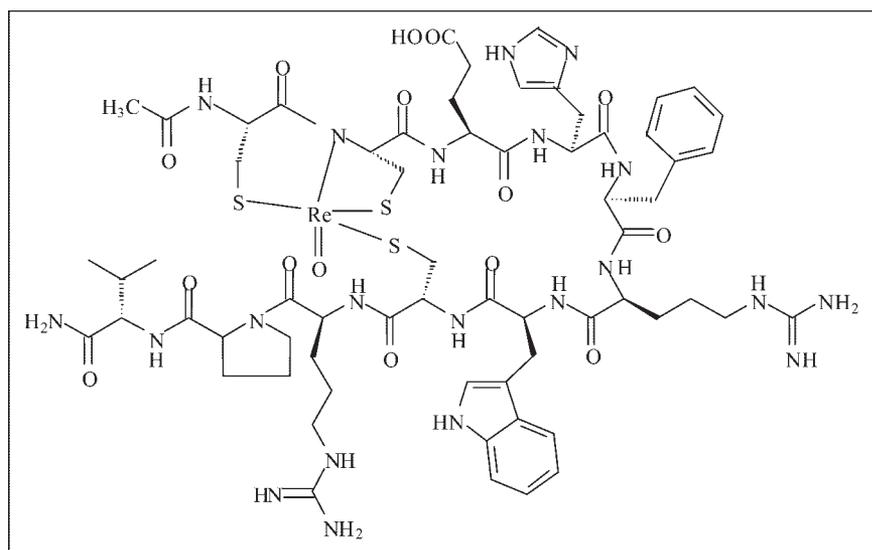

FIGURE 1. Structure of [188]ReO-(Arg[11])CCMSH: Ac-Cys-Cys-Glu-His-DPhe-Arg-Trp-Cys-Arg-Pro-Val-NH₂.

room temperature. Animal quality control results confirmed the biologic activity of the therapeutic dose of ^{188}Re-(Arg^{11})CCMSH.

The pharmacokinetics of ^{188}Re-(Arg^{11})CCMSH were determined from 5 min to 48 h in murine melanoma-bearing C57 mice for dosimetry calculation. Absorbed radioactivity doses to tumor and normal organs from ^{188}Re-(Arg^{11})CCMSH were estimated in this study based on the biodistribution data in B16/F1 murine melanoma-bearing mice. The results of mouse absorbed doses to tumor and normal organs are presented in Table 1. The absorbed dose to the B16/F1 mouse tumor was 3,022 cGy/37 MBq. The primary and secondary critical normal organs were large intestine and kidney, with absorbed doses of 1,462 cGy/37 MBq and 685 cGy/37 MBq, respectively. Two B16/F1 murine melanoma-bearing C57 mice were injected with ^{188}Re-(Arg^{11})CCMSH to visualize the tumors at 4 and 18 h after dose administration (Fig. 2). Although there was activity in the gastrointestinal system and kidney, melanoma tumors were visualized clearly at 4 h after injection. At 18 h after dose injection, extremely high tumor uptake and low background in the normal organs and tissues were demonstrated in the scintigraphic image, which is coincident with the pharmacokinetics of ^{188}Re-(Arg^{11})CCMSH.

Therapy studies were performed with C57 mice, inoculated subcutaneously with 1×10^6 B16/F1 cells in the right flank. Three days after tumor cell implantation, palpable dark melanoma tumors appeared. High-dose ^{188}Re-(Arg^{11})CCMSH treatment started on the fourth day after tumor cell inoculation. The effect of ^{188}Re-(Arg^{11})CCMSH treatment on the tumor growth rates and mean survival time of tumor mice are shown in Figures 3 and 4, respectively. We found that ^{188}Re-(Arg^{11})CCMSH yielded rapid and lasting therapeutic effects in the treatment groups. In contrast to the untreated control group, treatment groups with a single dose of 7.4 MBq, 22.2 MBq, or 2×14.8 MBq of ^{188}Re-(Arg^{11})CCMSH showed substantial tumor growth inhibition over the time
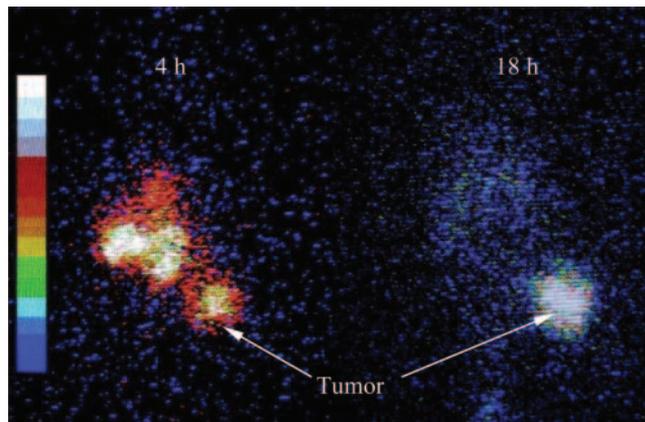

FIGURE 2. Melanoma imaging of ^{188}Re-(Arg^{11})CCMSH in B16/F1 murine melanoma-bearing C57 mice. Planar γ-camera images were collected 4 h (left) and 18 h (right) after administration of ^{188}Re-(Arg^{11})CCMSH.

period of the therapy study. For instance, on the third day after therapeutic dose administration, the average tumor volumes of the groups treated with 7.4 MBq, 22.2 MBq, and 2×14.8 MBq were 77.4%, 35.8%, and 54.7% of that of untreated control group, respectively. On the eighth day after dose injection, the average tumor volumes of the groups treated with 7.4 MBq, 22.2 MBq, and 2×14.8 MBq were 83.2%, 72.5%, and 59.2% of that of untreated control group. The therapeutic efficacy of ^{188}Re-(Arg^{11})CCMSH appeared to be dose dependent. The tumor growth rate decreased after a single dose of 22.2 MBq of ^{188}Re-(Arg^{11})CCMSH and was more pronounced than that of 7.4 MBq of ^{188}Re-(Arg^{11})CCMSH. The mice receiving the $2 \times$

TABLE 1
Radiation Absorbed Doses from ^{188}Re-(Arg^{11})CCMSH in B16/F1 Murine Melanoma-Bearing C57 Mice

Organ	cGy/37 MBq
Tumor	3,022.0
Kidney	685.0
Blood	240.0
Brain	37.8
Heart	131.0
Lung	172.0
Liver	135.0
Spleen	242.0
Stomach	284.0
Small intestine	570.0
Large intestine	1,462.0
Muscle	53.5
Pancreas	154.0

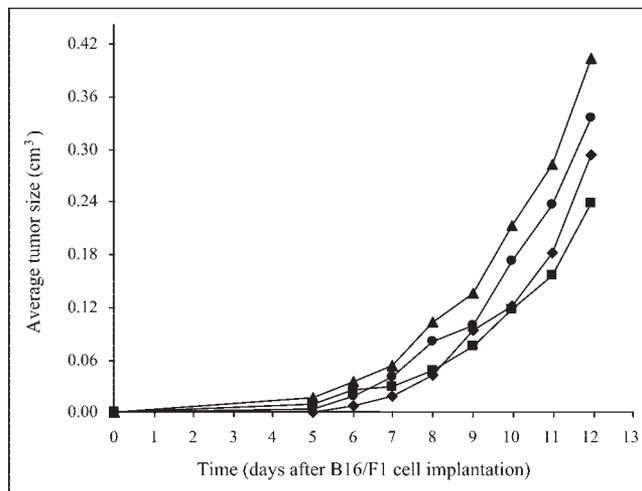**FIGURE 3.** Effect of ^{188}Re-(Arg^{11})CCMSH treatment on growth rate of B16/F1 murine melanoma tumors. Mice were implanted with B16/F1 tumor cells on day 0 and treated with ^{188}Re-(Arg^{11})CCMSH on day 4. Tumor measurements were performed daily starting 24 h after administration of 7.4 MBq (●), 22.2 MBq (◆), and 2×14.8 MBq (■) of ^{188}Re-(Arg^{11})CCMSH or saline placebo (▲). Second 14.8-MBq dose was given on day 7.
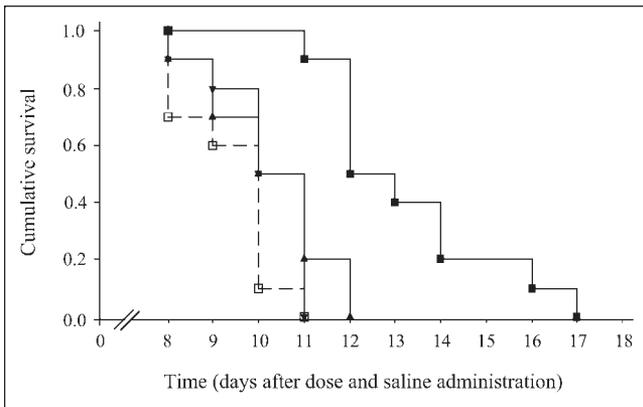
FIGURE 4. Survival analysis of B16/F1 murine melanoma-bearing C57 mice. Kaplan–Meier survival curves for B16/F1 murine melanoma-bearing mice treated with 7.4 MBq (▼), 22.2 MBq (▲), and 2 × 14.8 MBq (■) of ^{188}Re-(Arg^{11})CCMSH or saline placebo (□). Mean survival time was 9.4 ± 1.1 d for untreated control group, 10.2 ± 1.0 d ($P > 0.05$) for group treated with 7.4 MBq, 10.3 ± 1.3 d ($P > 0.05$) for group treated with 22.2 MBq, and 13.3 ± 1.9 d ($P < 0.05$) for group treated with 2 × 14.8 MBq.

FIGURE 5. Effect of ^{188}Re-(Arg^{11})CCMSH treatment on growth rate of TXM13 human melanoma tumors. Measurable TXM13 tumors were obtained on day 0 and treated with ^{188}Re-(Arg^{11})CCMSH on day 4. Tumor measurements were performed twice a week starting 4 d after administration of 22.2 MBq (▲), 2 × 14.8 MBq (●), and 37.0 MBq (■) of ^{188}Re-(Arg^{11})CCMSH or saline placebo (◆). Second 14.8 MBq dose was given on day 18.

14.8-MBq dose regimen of ^{188}Re-(Arg^{11})CCMSH exhibited the best overall tumor growth inhibition. The untreated control group exhibited unrestricted tumor growth and a mean survival time of 9.4 ± 1.1 d. The mean survival times were 10.2 ± 1.0 d and 10.3 ± 1.3 d for the groups treated with 7.4 MBq and 22.2 MBq of ^{188}Re-(Arg^{11})CCMSH, respectively. Although the single-dose treatment did extend the mean life of B16/F1 melanoma-bearing mice, the difference of mean survival time between the untreated control group and single-dose treated groups was not significant ($P > 0.05$; Fig. 4). On the other hand, the mean survival time of the group treated with the 2 × 14.8-MBq dose regimen was 13.3 ± 1.9 d, which was significantly longer than that of the untreated control group and single-dose treated groups ($P < 0.05$; Fig. 4). The results also demonstrated that multidose therapy was more effective than single-dose therapy.

The therapeutic efficacy of ^{188}Re-(Arg^{11})CCMSH was also examined in TXM13 human melanoma xenografted SCID mice. SCID mice received bilateral flank inoculations of 5 × 10^6 TXM13 tumor cells per site. Tumor-bearing mice were treated with ^{188}Re-(Arg^{11})CCMSH ~7 wk after tumor cell inoculation, when the tumors reached a measurable size (average size, 0.014 cm^3 in this study). The effects of ^{188}Re-(Arg^{11})CCMSH treatment on the tumor growth rates and mean survival time of tumor mice are shown in Figures 5 and 6, respectively. ^{188}Re-(Arg^{11})CCMSH administration exhibited rapid and lasting therapeutic effects in the treatment groups. In contrast to the untreated control group, treatment with a single dose of 37.0 MBq, 22.2 MBq, or 2 × 14.8 MBq of ^{188}Re-(Arg^{11})CCMSH resulted in substantial tumor growth inhibition over the time period of the therapy study. For example, on the eighth day after
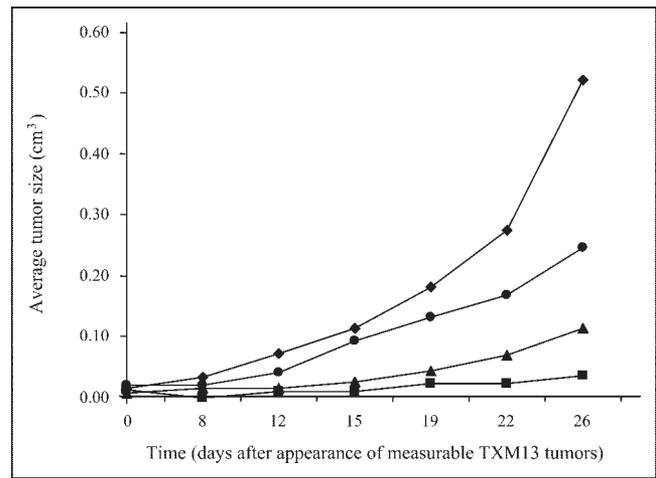
treatment, the average tumor volumes of groups treated with 37.0 MBq, 22.2 MBq, and 2 × 14.8 MBq were 11.4%, 20.0%, and 55.6% of that of the untreated control group. On the 22nd day after treatment, the average tumor volumes of groups treated with 37.0 MBq, 22.2 MBq, and 2 × 14.8 MBq were 6.5%, 21.5%, and 47.0% of those of the untreated control group. The therapeutic efficacy of ^{188}Re-(Arg^{11})CCMSH appeared to be radiation dose dependent. The decrease in tumor growth rate after a single dose of 37.0
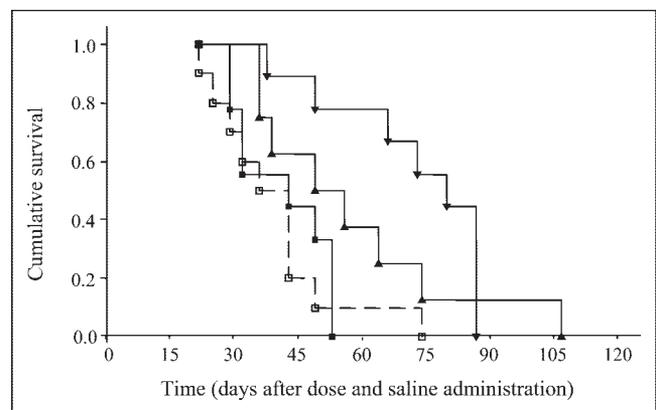

FIGURE 6. Survival analysis of TXM13 human melanoma-bearing SCID mice. Kaplan–Meier survival curves for TXM13 human melanoma-bearing mice treated with 22.2 MBq (▲), 2 × 14.8 MBq (■), and 37.0 MBq (▼) of ^{188}Re-(Arg^{11})CCMSH or saline placebo (□). Mean survival time was 39.6 ± 15.0 d for untreated control group, 41.4 ± 10.9 d ($P > 0.05$) for 2 × 14.8-MBq treated group, 57.6 ± 24.2 d ($P < 0.05$) for 22.2-MBq treated group, and 72.7 ± 18.3 d ($P < 0.05$) for 37.0-MBq treated group.

MBq of ^{188}Re-(Arg^{11})CCMSH was more pronounced than that of 22.2 MBq of ^{188}Re-(Arg^{11})CCMSH. In the human melanoma-bearing mice, a single dose of 37.0 MBq or 22.2 MBq of ^{188}Re-(Arg^{11})CCMSH was more effective in reducing the tumor growth rate than the 2×14.8-MBq fractionated dose. ^{188}Re-(Arg^{11})CCMSH treatment did increase the mean life expectancy of the TXM13 tumor xenografted SCID mice. For example, the untreated control group showed unrestricted tumor growth and the mean survival time was 39.6 ± 15.0 d, whereas the groups treated with 37.0 MBq, 22.2 MBq, and 2×14.8 MBq exhibited mean survival times of 72.7 ± 18.3, 57.6 ± 24.2, and 41.4 ± 10.9 d, respectively. The mean survival times between the control group and treatment groups were significantly different ($P < 0.05$; Fig. 6) for the 37.0-MBq and 22.2-MBq treatment groups but not significant ($P > 0.05$; Fig. 6) for the 14.8-MBq treatment group. One TXM13 tumor mouse in the 22.2-MBq treatment group survived the 100-d study period. The average weight of mice treated with ^{188}Re-(Arg^{11})CCMSH increased similarly to that of nontumor–bearing control mice and untreated tumor control mice except for the 37.0-MBq treatment group. The average weight of the group treated with 37.0 MBq decreased after the injection of the therapeutic dose and reached the nadir (81% of initial average weight) at the eighth day after dose injection. At the 15th day after injection, the average weight of the 37.0-MBq treated group was similar to the average weight of the nontumor–bearing control group, untreated tumor control group, and other treated groups. Throughout the study period, both treated mice and untreated tumor control mice maintained healthy physical appearance (without diarrhea and scruff coat). Comparison of hematology results between the untreated tumor control group and the group treated with 37.0 MBq showed that there was a significant decrease in WBC and RBC counts 1–2 wk after treatment and in platelet counts 1 wk after treatment ($P < 0.05$; Table 2). WBC, RBC, and platelet counts of the

treated group recovered by 3 wk after treatment. After the completion of therapy study, organs of interest, such as heart, kidney, liver, and stomach, were examined. Histopathologic examinations of heart, liver, and stomach showed no evidence of dose-related toxicity after high-dose ^{188}Re-(Arg^{11})CCMSH administration. The histopathologic profiles of kidneys of an untreated tumor control mouse and a B16/F1 tumor mouse treated with 2×14.8 MBq showed no overt signs of radiation toxicity to the kidneys with high-dose ^{188}Re-(Arg^{11})CCMSH treatment.

DISCUSSION

The prerequisite for radiolabeled receptor-avid peptides as therapeutic agents include therapeutic efficacy and favorable pharmacokinetics, such as rapid and high tumor uptake, extended tumor retention, high organ ratios of tumor to normal organ, and rapid whole-body clearance. ^{188}Re-(Arg^{11})CCMSH exhibited rapid receptor-mediated tumor uptake of 20.44 ± 1.91 percentage injected dose per gram (%ID/g) at 1 h after injection in murine melanoma-bearing C57 mice (33). Whole-body clearance of ^{188}Re-(Arg^{11})CCMSH was rapid, with ~90% of the activity cleared out of body through the urinary system at 4 h after injection. Significant tumor retention of ^{188}Re-(Arg^{11})CCMSH was demonstrated at 4 h after dose administration. For example, ~80% of the activity at 1 h after injection remained in the tumors at 4 h after infusion. Moreover, 24 h later, we observed 3.50 ± 2.32 %ID/g of ^{188}Re-(Arg^{11})CCMSH remaining in the tumors. The kidney was the major excretion pathway for ^{188}Re-(Arg^{11})CCMSH; however, renal clearance of ^{188}Re-(Arg^{11})CCMSH activity was rapid. Only 3.67 ± 0.51 %ID/g and 0.37 ± 0.11 %ID/g of ^{188}Re-(Arg^{11})CCMSH remained in the kidney at 4 and 24 h after injection, respectively (33).

Peptides and antibodies have been labeled with the high-energy β-particle emitters of ^{90}Y ($E_{\beta max} = 2.27$ MeV) and ^{188}Re ($E_{\beta max} = 2.11$ MeV) for targeted radiotherapy. The

TABLE 2
RBC, WBC, and Platelet Counts Comparison Between Untreated Tumor Control Group and Group
Treated with 37.0 MBq of ^{188}Re-(Arg^{11})CCMSH

Time (d)	RBC count (cells × 10^{12}/L)		WBC count (cells × 10^9/L)		Platelet count (platelets × 10^9/L)	
	Untreated	Treated	Untreated	Treated	Untreated	Treated
0	12.23 ± 0.91	11.12 ± 1.12*	9.56 ± 2.48	8.84 ± 1.42	827 ± 390	706 ± 309
8	11.92 ± 1.15	10.26 ± 1.18*	9.39 ± 2.20	3.34 ± 0.89*	796 ± 404	477 ± 69*
15	11.17 ± 1.69	9.17 ± 0.92*	7.54 ± 2.81	3.87 ± 1.38*	847 ± 258	842 ± 203
22	10.98 ± 1.10	11.15 ± 1.70	8.15 ± 3.66	7.55 ± 2.95	929 ± 407	702 ± 339
29	10.84 ± 1.14	9.51 ± 1.20*	7.49 ± 2.02	7.53 ± 3.02	662 ± 400	709 ± 243
36	10.01 ± 1.03	9.62 ± 0.93	8.68 ± 2.75	8.16 ± 1.33	820 ± 259	764 ± 240
43	10.34 ± 1.15	9.63 ± 1.64	8.63 ± 3.39	5.64 ± 0.83*	950 ± 383	868 ± 252

*$P < 0.05$.

RBC, WBC, and platelet counts on day 0 represent baseline counts before injection of ^{188}Re-(Arg^{11})CCMSH. Therapeutic dose of ^{188}Re-(Arg^{11})CCMSH was injected into mice on day 1.

maximum path length of β-particles emitted by [188]Re and ^{90}Y is ~11–12 mm (with mean path lengths of 4–5 mm), which permits the generation of a nearly homogeneous radiation dose to tumor cells even though the radioisotope maybe somewhat heterogeneously distributed throughout a tumor (*35*). In contrast to ^{90}Y, [188]Re has a 15% abundance 155-keV γ-ray, which is useful for imaging and dosimetry. The imageable γ-ray of [188]Re could be useful for determining individual patient dosimetry and for visualizing tumor uptake and retention with time. In this study, melanoma imaging of [188]Re-(Arg[11])CCMSH was performed in 2 B16 murine melanoma-bearing C57 mice at 4 and 18 h after infusion. The tumors were visualized clearly at 4 h after injection. At 18 h after dose injection, the high tumor uptake and low background in the normal organs and tissues were observed in the scintigraphic image.

This study demonstrated that [188]Re-(Arg[11])CCMSH produced therapeutic effects on both murine and human melanoma-bearing mice. In the B16/F1 murine melanoma mouse model, treatment with a single dosage of 7.4 MBq, 22.2 MBq, or 2 × 14.8 MBq of [188]Re-(Arg[11])CCMSH resulted in substantial tumor growth inhibition over the time period of the therapy study. However, a multiple-dose regimen of [188]Re-(Arg[11])CCMSH was more effective and exhibited the best overall tumor growth inhibition. Moreover, multiple-dose treatment of [188]Re-(Arg[11])CCMSH significantly extended the mean life expectancy of the B16/F1 tumor-bearing mice ($P < 0.05$; Fig. 4). Theoretically, a multiple-dose regimen may improve the therapeutic index of radiolabeled peptide by delivering a consistent tolerable radiation dose to the tumor over an extended period of time, while allowing intermittent recovery of dose-limiting normal organs. The advantages of a multiple-dose regimen over a single dose, such as improved therapeutic efficacy with decreased toxicity, have been demonstrated in radionuclide therapy with peptides (*9,38,39*). In the TXM13 human melanoma mouse model, single infusions of 22.2 MBq and 37.0 MBq of [188]Re-(Arg[11])CCMSH significantly extended the mean life expectancy of tumor-bearing mice ($P < 0.05$; Fig. 6), whereas 2 × 14.8 MBq failed to significantly improve survival ($P > 0.05$; Fig. 6). Both B16/F1 murine and TXM13 human melanoma tumors are highly aggressive and invasive; however, the TXM13 tumors grow at a slower rate than the B16/F1 tumors. Therefore, the interval between the two 14.8-MBq dose administrations of [188]Re-(Arg[11])CCMSH was different between B16/F1 and TXM13 tumor mouse models in this work. In the B16/F1 tumor therapy study, the interval between the 2 doses of 14.8 MBq of [188]Re-(Arg[11])CCMSH was 3 d, whereas the interval of 2 × 14.8 MBq of [188]Re-(Arg[11])CCMSH was 14 d in the TXM13 tumor mice therapy study. It appeared that 14 d might be too long to show the advantage of dose fractionation for TXM13 tumor therapy study.

We observed a significant difference in overall activity uptake between the B16/F1 murine melanoma tumors and the TXM13 human melanoma tumors in vivo. Tumor uptake of [188]Re-(Arg[11])CCMSH was 20.44 %ID/g and 3.50 %ID/g at 1 and 24 h after injection, respectively, in the B16 murine melanoma mice and 3.06 %ID/g and 0.93 %ID/g in the TXM13 human melanoma mice at the same time points (*33,34*). The differences in tumor uptake were attributed to lower receptor numbers per cell in the TXM13 human melanoma tumors and to the tumor morphology (*34*). On average, the TXM13 human melanoma cells had 1,500 fewer receptors per cell than the B16/F1 murine melanoma cells (5,500 vs. 7,000 receptors per cell). Histolopathologic analyses of the excised tumors revealed that murine melanoma tumors are highly vascularized gelatinous masses, whereas the human tumors formed solid masses with viable tumor cells surrounding a necrotic center that contained few identifiable melanoma cells (*32*). Administration of [188]Re-(Arg[11])CCMSH was effective in reducing tumor growth rates and extending mean survival times despite the differences in B16/F1 and TXM13 tumor uptake, morphology, and receptor number. Although the %ID/g of activity in the TXM13 human tumors was less than that in the B16/F1 murine tumors, it was most likely concentrated around the circumference of the tumor where viable melanoma cells were located in histologic studies (*32*). Much less activity would be expected in the necrotic center of the TXM13 tumors; however, the mass of the center would contribute significantly to the weight of the excised tumor and effectively reduce the overall %ID/g. This could explain why a 10-fold less uptake value in the TXM13 tumors resulted in therapeutic efficacies greater than or equal to that of the B16/F1 tumors.

Although administration of [188]Re-(Arg[11])CCMSH resulted in significant delays in both B16/F1 and TXM13 tumor growth, only one of the mice survived the entire 100-d study period. The survival results could be due to insufficient [188]Re-(Arg[11])CCMSH dose administration or to the fact that the tumor size was too small at the time of treatment with the high-energy β-particle emitter. Therapy studies with ^{90}Y-DOTA-octreotide analogs demonstrated complete responses of medium-sized CA20948 rat pancreatic tumors after administration of a 370-MBq dose (*40*). The estimated tumor dose for 1-g CA20948 tumors was 48 Gy, whereas the estimated tumor dose for 1-g B16/F1 tumors was 30.22 Gy. It is likely that melanoma therapy efficacy could be improved by higher administered dose. Receptor density of both B16/F1 and TXM13 cell lines will be a concern in higher dose therapy studies because the receptor numbers of both cell lines range from 5,500 to 7,000 per cell (*32*). However, HPLC purification after the radiolabeling reaction completely separated [188]Re-(Arg[11])CCMSH from the nonradiolabeled excess peptide, which might saturate the receptors in the tumors. In vitro competitive binding studies showed that the amount of nonradioactive Re-(Arg[11])CCMSH should be ~15–20 ng to

saturate the receptors of 5×10^5 B16/F1 or TXM13 cells, whereas the mass of 37.0 MBq of [188]Re-(Arg[11])CCMSH was 9.07 ng, which was less than the mass of peptide to saturate the receptors of 5×10^5 B16/F1 or TXM13 cells. Therefore, the therapeutic index of [188]Re-(Arg[11])CCMSH could be improved by higher dose. Nephrotoxicity of [188]Re-(Arg[11])CCMSH will be also a concern for higher dose therapy studies; however, L-lysine coinjection was shown to be effective in decreasing renal uptake of [188]Re-(Arg[11])CCMSH by 40% without impairing the tumor-targeting properties of [188]Re-(Arg[11])CCMSH (33). Therefore, L-lysine coinjection could be used to reduce the renal toxicity of higher doses of [188]Re-(Arg[11])CCMSH. Moreover, we found no apparent signs of toxicity related to high-dose [188]Re-(Arg[11])CCMSH. On the basis of dosimetry calculation results (Table 1), intestinal toxicity will be another concern for higher therapeutic dose. However, dose fractionation can be used to reduce the intestinal absorbed dose. Additionally, laxatives may also be used to help decrease the intestinal absorbed dose. The octreotide study also highlighted the relationship between tumor size and therapeutic efficacy (40). Treatment of medium-sized tumors ($\sim$8 cm^2) with [90]Y-DOTA-octreotide was more effective than treatment of small tumors ($\leq$1 cm^2), presumably because much of the decay energy was deposited outside the smaller size tumor volumes. Both the B16/F1 and TXM13 melanoma tumors were <1 cm^3 at the time of treatment. Like the therapy results with the ^{90}Y-DOTA-octreotide analogs in small tumors, it is possible that a significant fraction of the [188]Re disintegration energy would have been deposited outside the tumors.

CONCLUSION

This study demonstrated that [188]Re-(Arg[11])CCMSH treatment significantly decreased the tumor growth rate and extended the mean survival time of tumor-bearing mice in both the B16/F1 murine melanoma and the TXM13 human melanoma animals models. We did not observe signs of normal tissue toxicity related to high-dose [188]Re-(Arg[11])CCMSH administration. [188]Re-(Arg[11])CCMSH appears to be a promising radiolabeled peptide for targeted radionuclide therapy of melanoma.

REFERENCES

1. Jemal A, Tiwari RC, Murray T, et al. Cancer statistics, 2004. *CA Cancer J Clin.* 2003;54:8–29.
2. Marghoob AA, Slade J, Salopek TG, Kopf AW, Bart RS, Rigel DS. Basal cell and squamous cell carcinomas are important risk factors for cutaneous malignant melanoma. *Cancer.* 1995;75:707–714.
3. Anderson CM, Buzaid AC. Systematic treatments for advanced cutaneous melanoma. *Oncology.* 1995;9:1149–1158.
4. Heppeler A, Froidevaux S, Eberle AN, Maecke HR. Receptor targeting for tumor localization and therapy with radiopeptides. *Curr Med Chem.* 2000;7:971–994.
5. Volkert WA, Goeckeler WF, Ehrhardt GJ, Ketring AR. Therapeutic radionuclides: production and decay property consideration. *J Nucl Med.* 1991;32:174–185.
6. Otte A, Jermann E, Behe M, et al. A powerful new tool for receptor-mediated radionuclide therapy. *Eur J Nucl Med.* 1997;24:792–795.
7. Otte A, Mueller-Brand J, Dellas S, Nitzsche EU, Herrmann R, Maecke HR. Yttrium-90-labelled somatostatin-analogue for cancer treatment. *Lancet.* 1998;351:417–418.
8. Zamora PO, Bender H, Gulhke S, et al. Pre-clinical experience with Re-188-RC-160, a radiolabeled somatostatin analog for use in peptide-targeted radiotherapy. *Anticancer Res.* 1997;17:1803–1808.
9. de Jong M, Breeman WAP, Bernard BF, et al. [^{177}Lu-DOTA[0],Tyr[3]]octreotate for somatostatin receptor-targeted radionuclide therapy. *Int J Cancer.* 2001;92:628–633.
10. Freitas JE, Gross MD, Ripley S, Shapiro B. Radionuclide diagnosis and therapy of thyroid cancer: current status report. *Semin Nucl Med.* 1985;15:106–131.
11. Hoefnagel CA. Radionuclide therapy revisited. *Eur J Nucl Med.* 1991;18:408–431.
12. Bakker WH, Albert R, Bruns C, et al. (111-In-DTPA-D-Phe[1])-octreotide, a potential radiopharmaceutical for imaging of somatostatin receptor-positive tumors: synthesis, radiolabeling and in vitro validation. *Life Sci.* 1991;49:1583–1591.
13. Krenning EP, Bakker WH, Kooij PPM, et al. Somatostatin receptor scintigraphy with [^{111}In-DTPA-D-Phe[1]]-octreotide in man: metabolism, dosimetry and comparison with [^{123}I-Tyr[3]]-octreotide. *J Nucl Med.* 1992;33:652–658.
14. Krenning EP, Kwekkeboom DJ, Bakker WH, et al. Somatostatin receptor scintigraphy with [In-111-DTPA-D-Phe] and [I-123-Tyr-3]octreotide: the Rotterdam experience with more than 1000 patients. *Eur J Nucl Med.* 1993;20:716–731.
15. Chinol M, Bodei L, Cremonesi M, Paganelli G. Receptor-mediated radiotherapy with Y-DOTA-dPhe-Tyr-octreotide: the experience of the European Institute of Oncology Group. *Semin Nucl Med.* 2002;32:141–147.
16. Paganelli G, Zoboli S, Cremonesi M, et al. Receptor mediated radiotherapy with ^{90}Y-DOTA-d-Phe[1]-Tyr[3]-octreotide. *Eur J Nucl Med.* 2001;28:426–434.
17. Waldherr C, Pless M, Maecke HR, et al. Tumor response and clinical benefit in neuroendocrine tumors after 7.4 GBq ^{90}Y-DOTATOC. *J Nucl Med.* 2002;43:610–616.
18. de Jong M, Valkema R, Jamar F, et al. Somatostatin receptor-targeted radionuclide therapy of tumors: preclinical and clinical findings. *Semin Nucl Med.* 2002;32:133–140.
19. Hruby VJ, Sharma SD, Toth K, et al. Design, synthesis, and conformation of superpotent and prolonged acting melanotropins. *Ann NY Acad Sci.* 1993;680:51–63.
20. Tatro JB, Reichlin S. Specific receptors for alpha-melanocyte-stimulating hormone are widely distributed in tissues of rodents. *Endocrinology.* 1987;121:1900–1907.
21. Siegrist W, Solca F, Stutz S, et al. Characterization of receptors for alpha-melanocyte-stimulating hormone on human melanoma cells. *Cancer Res.* 1989;49:6352–6358.
22. Tatro JB, Wen Z, Entwistle ML, et al. Interaction on an α-melanocyte stimulating hormone-diptheria toxin fusion protein with melanotropin receptors in human metastases. *Cancer Res.* 1992;52:2545–2548.
23. Sawyer TK, Sanfilippo PJ, Hruby VJ, et al. [Nle[4],D-Phe[7]]α-melanocyte stimulating hormone: a highly potent α-melanotropin with ultralong biological activity. *Proc Natl Acad Sci USA.* 1980;77:5754–5758.
24. Bard DR, Knight CG, Page-Thomas DP. A chelateing derivative of α-melanocyte stimulating hormone as a potential imaging agent for malignant melanoma. *Br J Cancer.* 1990;62:919–922.
25. Bagutti C, Stolz B, Albert R, Bruns C, Pless J, Eberle AN. ^{111}In-DTPA-labeled analogs for alpha-melanocyte-stimulating hormone for melanoma targeting: receptor binding in vitro and in vivo. *Int J Cancer.* 1994;58:749–755.
26. Wraight EP, Bard DR, Maughan CG, Knight CG, Page-Thomas DP. The use of

a chelating derivative of alpha-melanocyte stimulating hormone for the clinical imaging of malignant melanoma. *Br J Radiol.* 1992;65:112–118.

27. Vaidyanathan G, Zalutsky MR. Fluorine-18-labeled [Nle⁴,D-Phe⁷]-α-MSH, an α-melanocyte stimulating hormone analog. *Nucl Med Biol.* 1997;24:171–178.

28. Froidevaux S, Calame-Christe M, Tanner H, Sumanovski L, Eberle AN. A novel DOTA-α-melanocyte-stimulating hormone analog for metastatic melanoma diagnosis. *J Nucl Med.* 2002;43:1699–1706.

29. Froidevaux S, Calame-Christe M, Schuhmacher J, et al. A gallium-labeled DOTA-α-melanocyte-stimulating hormone analog for imaging of melanoma metastases. *J Nucl Med.* 2004;45:116–123.

30. Giblin MF, Jurisson SS, Quinn TP. Synthesis and characterization of rhenium-complexed α-melanotropin analogs. *Bioconjug Chem.* 1997;8:347–353.

31. Giblin MF, Wang NN, Hoffman TJ, Jurisson SS, Quinn TP. Design and characterization of α-melanotropin peptide analogs cyclized through rhenium and technetium metal coordination. *Proc Natl Acad Sci USA.* 1998;95:12814–12818.

32. Chen J, Cheng Z, Hoffman TJ, Jurisson SS, Quinn TP. Melanoma-targeting properties of ⁹⁹ᵐtechnetium-labeled cyclic α-melanocyte-stimulating hormone peptide analogues. *Cancer Res.* 2000;60:5649–5658.

33. Miao Y, Owen NK, Whitener D, Gallazzi F, Hoffman TJ, Quinn TP. In vivo evaluation of ¹⁸⁸Re-labeled alpha-melanocyte stimulating hormone peptide analogs for melanoma therapy. *Int J Cancer.* 2002;101:480–487.

34. Miao Y, Whitener D, Feng W, Owen NK, Chen J, Quinn TP. Evaluation of the human melanoma targeting properties of radiolabeled alpha-melanocyte stimulating hormone peptide analogues. *Bioconjug Chem.* 2003;14:1177–1184.

35. Schubiger PA, Alberto R, Smith A. Vehicles, chelators, and radionuclides: choosing the "building blocks" of an effective therapeutic radioimmunoconjugate. *Bioconjug Chem.* 1996;7:165–179.

36. Hui TE, Fisher DR, Kuhn JA, et al. A mouse model for calculating cross-organ beta doses from yttrium-90-labeled immunoconjugates. *Cancer.* 1994;73(suppl):951–957.

37. Beatty BG, Kuhn JA, Hui TE, Fisher DR, Williams LE, Beatty JD. Application of the cross-organ beta dose method for tissue dosimetry in tumor-bearing mice treated with a ⁹⁰Y-labeled immunoconjugate. *Cancer.* 1994;73(suppl):958–965.

38. Anderson CJ, Jones LA, Bass LA, et al. Radiotherapy, toxicity and dosimetry of copper-64-TETA-octreotide in tumor-bearing rats. *J Nucl Med.* 1998;39:1944–1951.

39. Lewis JS, Lewis MR, Cutler PD, et al. Radiotherapy and dosimetry of ⁶⁴Cu-TETA-Tyr³-octreotate in a somatostatin receptor-positive, tumor-bearing rat model. *Clin Cancer Res.* 1999;5:3608–3616.

40. de Jong M, Breeman WAP, Bernard BF, et al. Tumor response after [⁹⁰Y-DOTA⁰,Tyr³]-octreotide radionuclide therapy in a transplantable rat tumor model is dependent on tumor size. *J Nucl Med.* 2001;42:1841–1846.